

Lightweight SAR Ship Detection via Contrastive Distillation

Surendar Devasundaram
University of Arizona
Department of Electrical and
Computer Engineering
Tucson, Arizona, USA
surdev@arizona.edu

Banafsheh Saber Latibari
University of Arizona
Department of Electrical and
Computer Engineering
Tucson, Arizona, USA
banafsheh@arizona.edu

Abhijit Mahalanobis
University of Arizona
Department of Electrical and
Computer Engineering
Tucson, Arizona, USA
amahalan@arizona.edu

Abstract

Deep convolutional and transformer-based detectors achieve strong performance for SAR ship detection but are often computationally prohibitive for real-time or onboard deployment. Lightweight models offer improved efficiency yet struggle to capture the complex structural relationships inherent in SAR backscatter. Most existing SAR knowledge-distillation approaches rely on feature or logit matching, which enforces localized activation similarity while neglecting the geometric relationships among object representations. We propose a **Structured Unified Relational knowlGE** distillation framework for **SAR Ship** detection (**SURGE**) that transfers relational geometry from a powerful teacher detector to a compact student detector using a contrastive InfoNCE objective in a shared projection embedding space. To the best of our knowledge, this work presents the first transformer-based SAR ship detector knowledge distillation framework in SAR domain. The framework is architecture-agnostic in the sense that it provides a common region-level distillation interface for two-stage, one-stage and transformer-based detectors without modifying their deployed architectures. Experiments on the SSDD and HRSID benchmarks demonstrate that the proposed method yields substantial improvements for two-stage detectors, achieving up to **6.2 mAP** and **8.0 AP₇₅** gains over baseline student and even surpassing teacher performance.

CCS Concepts: • **Computing methodologies** → **Computer vision problems.**

Keywords: Synthetic Aperture Radar (SAR), Ship Detection, Contrastive Distillation, Object Detection, Knowledge Distillation

1 Introduction

Synthetic Aperture Radar (SAR) imaging enables robust object detection under adverse weather and illumination conditions, making it indispensable for maritime surveillance,

disaster management, and defense applications. Unlike optical imagery, SAR captures backscattering responses from surface structures, providing critical geometric and material information even through clouds and darkness [12]. However, the strong speckle noise, complex scattering mechanisms, and fine structural variations of SAR scenes pose unique challenges for deep object detectors [24].

High-capacity convolutional and transformer-based detectors such as Faster R-CNN [5], RetinaNet [10], and DETR [1] achieve strong detection accuracy, and their adaptation to SAR data has yielded high-performing but computationally expensive models [3, 4, 9]. Such models are often unsuitable for real-time or onboard deployment due to memory and latency constraints. In contrast, lightweight detectors improve efficiency but frequently lose discriminative power, struggling to capture the structural relationships that distinguish targets from clutter in SAR backscatter. Knowledge distillation (KD) has been explored to transfer knowledge from large teacher models to compact students. However, *existing SAR-oriented KD methods primarily rely on feature-map matching* [11, 16] or *logit alignment* [6, 17], enforcing localized activation similarity. These approaches do not explicitly model the relational geometry that governs how a teacher organizes object representations in feature space. As a result, the student learns local responses rather than the structural reasoning employed by the teacher—an important limitation in SAR imagery, where contextual and geometric cues are critical. We address this limitation by proposing a relation-aware knowledge distillation framework that transfers object-level relational geometry from a teacher detector to a compact student. Our method formulates distillation as a contrastive Information Noise-Contrastive Estimation (InfoNCE) objective in a shared projection embedding space, where normalized teacher and student region features are compared via pairwise similarity. We emphasize that the novelty is not a new general-purpose contrastive objective, but a detection-aware formulation for SAR ship detection: teacher predictions from heterogeneous detector families are converted into candidate object regions, aligned across teacher and student preprocessing spaces, and used to supervise object/region embeddings rather than whole-image representations or local activation maps. This enables an architecture-agnostic region-level distillation interface for

arXiv:2605.30380v2 [cs.CV] 1 Jun 2026



This work is licensed under a Creative Commons Attribution 4.0 International License.

two-stage, one-stage, and transformer-based detectors while encouraging the student to preserve the teacher’s semantic topology instead of merely matching pixel-level or activation-level responses. Among the evaluated detector families, the two-stage Faster R-CNN architecture is the strongest choice for SAR ship detection and SURGE provides its most substantial improvement on this family. Our main contributions are summarized as follows:

- We propose **SURGE**, a unified relation-aware knowledge distillation framework for SAR ship detection. The novelty lies in converting heterogeneous detector predictions into aligned candidate regions and transferring relational geometry among object-level embeddings, rather than introducing a new general-purpose InfoNCE loss.
- We introduce a **unified region-level distillation interface** applicable to two-stage, one-stage, and transformer-based detectors without modifying their core designs.
- To the best of our knowledge, we present the first transformer-based distillation framework for SAR ship detection, demonstrating effective relational transfer without relying on query-level supervision.
- Experiments on SSDD and HRSID show substantial gains for lightweight two-stage detectors, with up to **6.2 mAP** and **8.0 AP₇₅** improvement while achieving over **50% parameter reduction**.

2 Related Works

Recent work in SAR ship detection has primarily focused on adapting deep object detectors originally developed for optical imagery [7]. Two-stage detectors such as Faster R-CNN[9] and one-stage architectures, including RetinaNet [4] have been extended to SAR data using multiscale feature learning and task-specific preprocessing to mitigate speckle noise and complex scattering effects. More recently, transformer-based detectors inspired by DETR have been explored to leverage global context modeling in SAR imagery [22]. While these approaches achieve strong detection accuracy, their reliance on deep backbones and dense feature representations results in high computational complexity, limiting their suitability for real-time or onboard SAR systems. Knowledge distillation has been investigated to reduce the computational cost of deep models in SAR recognition and detection tasks [11, 16]. Existing SAR-oriented distillation methods predominantly rely on feature-map matching or output-level logit alignment [18, 21, 23]. Representative approaches transfer intermediate convolutional features using attention mechanisms, multiscale supervision, or privileged information [8], and some combine distillation with network pruning or lightweight architectural design. Despite their effectiveness, these methods primarily enforce localized activation similarity and do not explicitly capture the relational structure among object representations, with most studies focusing on target recognition or classification rather than

architecture-agnostic SAR ship detection. Relation-aware KD has been proposed in general computer vision to preserve structural information in representation spaces [13, 15]. By transferring pairwise similarities or distances, these methods enable students to learn the geometric organization of teacher embeddings. More recently, contrastive objectives such as InfoNCE have been incorporated into distillation frameworks [14, 19], improving robustness and generalization in optical image classification and detection. However, to our knowledge, relation-aware contrastive distillation has not been systematically studied for SAR ship detection across heterogeneous detector architectures, motivating the unified region-level framework proposed in this work.

3 Methodology

Our SURGE framework is depicted in Fig. 1, where the teacher and student detectors process the same input SAR image to extract multi-scale feature maps. High-confidence predictions from the frozen teacher are decoded into candidate regions, which are spatially aligned with the student and used to extract corresponding region features via RoIAlign. These aligned region features are projected into a shared embedding space and supervised using a contrastive objective, while the student is simultaneously optimized with the standard detection loss. Despite architectural differences as shown in Fig. 2, all detectors ultimately produce classification and localization outputs, which enables a unified region-level distillation strategy that preserves the geometric structure of the teacher’s representation space.

Teacher-Guided Region Generation: Given an input image x , the teacher detector produces a set of candidate regions $\mathcal{R} = \{r_i\}_{i=1}^N$, each associated with a semantic label c_i and a localization quality score IoU_i computed with respect to ground truth. These regions serve as anchors for object-level distillation. For two-stage detectors, regions are obtained directly from the teacher’s region proposal network (RPN). For one-stage detectors, high-confidence predictions are selected from dense outputs, decoded into bounding boxes, and treated as pseudo-proposals. For detection transformers, high-confidence bounding boxes predicted by the teacher DETR decoder are used as candidate regions. In all cases, the resulting regions are used to extract region-level features via RoIAlign, providing a unified interface across detector paradigms.

Cross-Detector Feature Alignment: Teacher-derived regions are first mapped back to the ground-truth image coordinate system and then transformed into the student image space to account for architectural differences in preprocessing.

Relation-Aware Distillation Objective: Let f_i^T and f_i^S denote the teacher and student region features corresponding to region r_i . Region features are globally pooled and

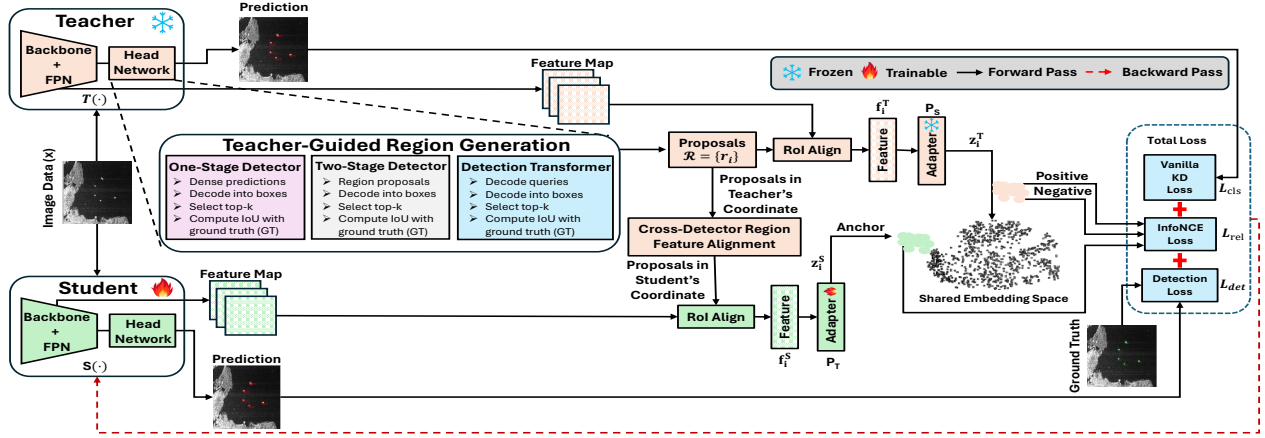


Figure 1. Overview of SURGE framework for SAR ship detection. Given an input SAR image x , a frozen teacher detector $T(\cdot)$ and a trainable student detector $S(\cdot)$ extract feature maps using a backbone and FPN. Teacher predictions are decoded into candidate regions $\mathcal{R} = \{r_i\}$ (region proposals for two-stage detectors, dense predictions for one-stage detectors or decoder-predicted bounding boxes in DETR), followed by top- K selection and IoU-based filtering. Teacher regions are mapped to the student image space to ensure spatial alignment, and RoI features f_i^T and f_i^S are extracted via RoIAlign and projected using heads P_T and P_S to obtain normalized embeddings z_i^T and z_i^S . The student is trained by jointly optimizing the detection loss \mathcal{L}_{det} , vanilla distillation losses, and a relation-aware contrastive loss \mathcal{L}_{rel} based on an InfoNCE objective, encouraging preservation of the teacher’s relational geometry across detector architectures.

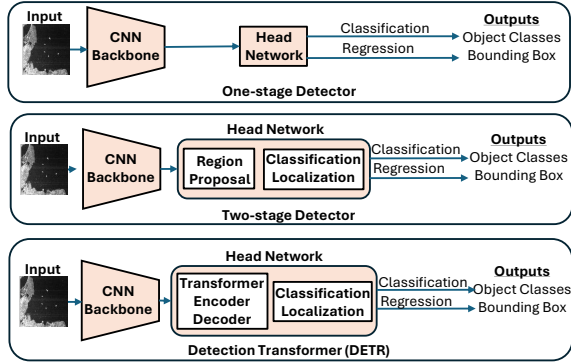


Figure 2. Head network designs for different object detection paradigms. **Top: One-stage detectors** directly predict class scores and bounding boxes from dense backbone feature maps. **Middle: Two-stage detectors** generate region proposals via an RPN, followed by per-proposal classification and localization heads. **Bottom: Detection transformers** process CNN features with a transformer encoder–decoder, where object queries are decoded to jointly predict class labels and bounding boxes.

projected into a shared embedding space:

$$z_i^T = \frac{P_T(\text{GAP}(f_i^T))}{\|P_T(\text{GAP}(f_i^T))\|}, \quad z_i^S = \frac{P_S(\text{GAP}(f_i^S))}{\|P_S(\text{GAP}(f_i^S))\|}, \quad (1)$$

where $\text{GAP}(\cdot)$ denotes global average pooling, P_T and P_S are lightweight projection heads, and embeddings are L2-normalized. For each student embedding z_i^S , positive and negative sets (In all experiments, we use $\tau_{pos} = 0.5$ and

$\tau_{neg} = 0.3$) are defined using teacher-derived semantic and localization cues:

$$\mathcal{P}(i) = \{j \mid c_j = c_i, \text{IoU}_j \geq \tau_{pos}\}, \quad (2)$$

$$\mathcal{N}(i) = \{j \mid \text{IoU}_j \leq \tau_{neg}\}. \quad (3)$$

A student-anchored InfoNCE objective is used to preserve the relational geometry of the teacher representation:

$$\mathcal{L}_{rel} = -\frac{1}{|\mathcal{A}|} \sum_{i \in \mathcal{A}} \log \frac{\sum_{j \in \mathcal{P}(i)} \exp(\text{sim}(i, j))}{\sum_{j \in \mathcal{P}(i) \cup \mathcal{N}(i)} \exp(\text{sim}(i, j))}, \quad (4)$$

where \mathcal{A} denotes anchors with at least one valid positive, and $\text{sim}(i, j)$ is the temperature-scaled cosine similarity between the student anchor embedding and the teacher region embedding. To stabilize training, the number of positives is capped and hard negative mining is applied. The use of InfoNCE is motivated by the multi-positive/multi-negative structure of the proposed supervision. Unlike one-to-one feature regression, the objective encourages a student region embedding to preserve the relative neighborhood structure induced by teacher-derived semantic and localization cues. Thus, the goal is relative separation and relational geometry preservation rather than direct activation matching. In addition to relational distillation, standard output-level distillation is applied to classification and bounding-box predictions for convolutional detectors. For two-stage detectors, this supervision is applied at the RoI head, while for one-stage detectors it is applied to dense prediction heads. For detection transformers, output-level distillation is not employed, as the unordered set-based predictions lead to unstable teacher–student correspondence and were observed

to degrade performance. Consequently, DETR models rely exclusively on region-level relational distillation. The overall training objective is defined in eq where \mathcal{L}_{det} is the standard detection loss and λ terms balance the contributions of relational, classification, and localization distillation.

$$\mathcal{L} = \mathcal{L}_{\text{det}} + \lambda_c \mathcal{L}_{\text{rel}} + \lambda_{\text{cls}} \mathcal{L}_{\text{cls}}^{\text{KD}} + \lambda_{\text{box}} \mathcal{L}_{\text{box}}^{\text{KD}}. \quad (5)$$

4 Experimental Setup

We evaluate the proposed framework on two public SAR ship detection benchmarks: the **SSDD** and the **HRSID**. SSDD images are resized to 512×512 , while HRSID images are resized to 800×800 . Official train/test splits are used in all experiments. Performance is measured using COCO-style mean Average Precision (mAP), along with AP_{50} and AP_{75} . Experiments are conducted on two-stage, one-stage, and transformer-based detectors. For two-stage detection, Faster R-CNN with a ResNet-101 backbone is used as the teacher and ResNet-18 as the student. For one-stage detection, RetinaNet with ResNet-101 (teacher) and ResNet-18 (student) backbones is employed. For transformer-based detection, DETR with a ResNet-101 teacher and a ResNet-50 student is used. All models follow their standard architectural definitions, and distillation is applied externally without modifying detector designs. Teacher and student networks are initialized from ImageNet-pretrained weights, with teacher parameters frozen during distillation. Relation-aware KD is implemented using a student-anchored InfoNCE loss defined over region-level features. Positive and negative pairs are selected based on teacher-derived semantic labels and IoU thresholds, with temperature scaling, capped positives, and hard negative mining applied for stability. For convolutional detectors, standard logit-level and bounding-box distillation losses are additionally used, while for DETR, we do not apply direct query-level supervision (output-level distillation), where teacher and student decoder queries or output slots are matched one-to-one. DETR predictions are unordered set outputs, and direct teacher-student alignment at the decoder-query level can produce unstable correspondences. Instead, teacher-decoded boxes are treated as region anchors, mapped into student image space, and used for RoI-based relational distillation. Consequently, DETR models rely exclusively on region-level relational distillation in our framework. All models are implemented in PyTorch. Faster R-CNN models are trained using SGD with momentum 0.9 and weight decay 1×10^{-4} , while RetinaNet and DETR models use AdamW with the same weight decay. Convolutional detectors are trained for 50 epochs with a multi-step learning rate schedule (decay at epochs 15 and 30), while DETR models are finetuned for 300 epochs to account for slower convergence. Batch size is set to 4 across all experiments. All training is performed on a single NVIDIA L40S GPU.

5 Results

Table 1 summarizes the performance of teacher, student, and distilled models across two-stage, one-stage, and transformer-based detectors on the SSDD and HRSID datasets, together with their parameter counts. The comparison reveals that Faster R-CNN family achieves the strongest overall performance for SAR ship detection, and SURGE yields its largest gains on this best-performing detector family. All convolution-based detector results are reported using COCO-style metrics and averaged over six independent runs while DETR’s is averaged over two independent runs. For comparison, we implemented a baseline KD[2] based on standard object detection distillation from the RGB domain, applying output-level teacher-student supervision.

While several SAR-specific KD methods have been proposed [11, 16, 18], their implementations are not publicly available and largely rely on localized feature or logit alignment. The adopted baseline thus serves as a fair and reproducible reference for evaluation. The proposed relation-aware distillation yields the most significant improvements for two-stage detectors. On SSDD, the Faster R-CNN student with a ResNet-18 backbone improves from 62.87 mAP to 68.03 mAP, corresponding to a gain of +5.16 mAP over the non-distilled student and +0.27 mAP over baseline distillation. Notably, the distilled student surpasses the ResNet-101 teacher by +1.33 mAP while using approximately 51% fewer parameters, demonstrating that relational geometry transfer can compensate for reduced model capacity. Similar trends are observed on HRSID, where the proposed method improves the student by +6.03 mAP and +7.71 AP_{75} , highlighting substantial gains in localization accuracy. While baseline distillation already improves performance over the student, the proposed relation-aware objective consistently provides larger gains, particularly at higher IoU thresholds. These results indicate that preserving inter-region relationships is especially beneficial for two-stage detectors, which explicitly model object-level representations through region proposals. On SSDD, the proposed method for one-stage RetinaNet model yields comparable AP_{75} performance but slightly lower mAP than both the baseline student and conventional distillation; however, this difference falls within the margin of statistical variability (the student model achieves 61.12 ± 0.72 mAP (95% CI: [60.36, 61.88]), vanilla knowledge distillation achieves 60.74 ± 0.36 mAP (95% CI: [60.36, 61.11]), and the proposed method achieves 60.33 ± 0.81 mAP (95% CI: [59.48, 61.18])). The substantial overlap of confidence intervals indicates that the observed performance differences are not statistically significant.) On HRSID, however, the proposed method improves the student by +0.65 mAP and +1.10 AP_{75} , indicating that relational distillation can still provide benefits in more complex scenes with higher object density. Compared to two-stage detectors, the smaller gains for one-stage models can be attributed to the absence of explicit

Table 1. Performance comparison of CNN-based and transformer-based detectors on SSDD and HRSID. Results are mean \pm std across 6 runs (1 & 2 stage) and across 2 runs (Transformer). Δ denotes change relative to the non-distilled student (mean values). Bold indicates the best student performance per detector.

Detector	Model	Params (M)	SSDD			HRSID		
			mAP	AP ₅₀	AP ₇₅	mAP	AP ₅₀	AP ₇₅
Two-Stage (Faster R-CNN)	R101 (Teacher)	63.8	66.70 \pm 0.33	93.50 \pm 0.80	82.26 \pm 0.80	62.09 \pm 0.11	86.36 \pm 0.07	70.76 \pm 0.33
	R18 (Student)	31.2	62.87 \pm 0.49	91.08 \pm 0.75	74.64 \pm 1.28	59.93 \pm 0.19	84.65 \pm 0.07	69.01 \pm 0.34
	R18 + Vanilla KD	31.2	67.76 \pm 0.66	93.81 \pm 0.87	81.78 \pm 1.12	65.98 \pm 0.10	87.06 \pm 0.33	77.21 \pm 0.43
	R18 + Proposed RKD	31.2	68.03 \pm 1.35	94.13 \pm 0.97	82.35 \pm 1.63	65.96 \pm 0.16	88.10 \pm 0.51	76.72 \pm 0.40
	Δ Student \rightarrow RKD	-	+5.16	+3.05	+7.71	+6.03	+3.45	+7.71
One-Stage (RetinaNet)	R101 (Teacher)	56.6	60.99 \pm 0.81	92.61 \pm 1.25	72.11 \pm 1.19	62.68 \pm 0.27	88.91 \pm 0.28	71.39 \pm 0.35
	R18 (Student)	23.5	61.12 \pm 0.72	93.73 \pm 1.08	70.72 \pm 1.62	62.12 \pm 0.28	89.03 \pm 0.36	71.02 \pm 0.44
	R18 + Vanilla KD	23.5	60.74 \pm 0.36	94.10 \pm 0.81	70.99 \pm 0.76	63.21 \pm 0.50	89.47 \pm 0.65	73.01 \pm 0.58
	R18 + Proposed RKD	23.5	60.33 \pm 0.81	93.67 \pm 0.52	70.65 \pm 1.48	62.77 \pm 0.33	89.36 \pm 0.53	72.12 \pm 0.40
	Δ Student \rightarrow RKD	-	-0.79	-0.06	-0.07	+0.65	+0.33	+1.10
Transformer (DETR)	R101 (Teacher)	60.3	59.33 \pm 1.62	90.85 \pm 2.58	69.61 \pm 1.84	50.49 \pm 0.10	74.20 \pm 0.86	58.16 \pm 0.65
	R50 (Student)	41.3	59.37 \pm 0.00	91.47 \pm 0.73	68.94 \pm 0.36	48.77 \pm 0.12	72.87 \pm 0.18	56.14 \pm 0.59
	R50 + Proposed RKD	41.3	59.70 \pm 0.57	91.59 \pm 0.46	69.02 \pm 0.44	48.60 \pm 0.19	73.04 \pm 0.15	55.95 \pm 0.10
	Δ Student \rightarrow RKD	-	+0.33	+0.12	+0.08	-0.17	+0.17	-0.19

region proposals and the reliance on dense anchor-based predictions, which may restrict the expressiveness of region-level relational supervision. For transformer-based detectors, we evaluate DETR using a region-based distillation strategy derived from teacher-predicted bounding boxes. Although the absolute gains are smaller, the proposed method consistently improves the student model, achieving +0.33 mAP over the baseline student and marginal improvements over the teacher. A conventional output-level distillation baseline is not reported for DETR, as its unordered set-based predictions lack a stable teacher-student correspondence and led to degraded performance in our preliminary experiments. The results confirm that relational knowledge can be effectively transferred to transformer-based detectors through a unified RoI-based interface, even when query-level supervision is not explicitly used.

Loss Ablation: Table 2 presents an ablation study analyzing the contribution of different loss components. Vanilla KD alone yields substantial gains over detection-only training, while relational distillation alone provides limited improvement. The strongest performance is achieved when relational distillation is combined with vanilla KD, resulting in a +5.16 mAP and +7.71 AP₇₅ improvement over the detection-only baseline. These results demonstrate that relational supervision is most effective when complementing conventional teacher-student distillation rather than replacing it.

Computational Efficiency: Since the proposed method is used only during training, it does not modify the deployed student detector. Therefore, computational cost is identical for the baseline student, vanilla KD student, and SURGE student within the same detector family. SURGE adds

Table 2. Loss ablation on **Faster R-CNN R18 (SSDD)**. Mean \pm std over $n = 6$ runs.

Losses Used	mAP	AP ₅₀	AP ₇₅
Det only	62.87 \pm 0.49	91.08 \pm 0.75	74.64 \pm 1.28
Det + KD	67.76 \pm 0.66	93.81 \pm 0.87	81.78 \pm 1.12
Det + Rel	62.77 \pm 0.33	89.36 \pm 0.53	72.12 \pm 0.40
Det + KD + Rel (Ours)	68.03 \pm 1.35	94.13 \pm 0.97	82.35 \pm 1.63

training-only overhead from teacher inference, region decoding, RoAlign, and projection heads, but leaves deployment-time latency and memory unchanged. We report GFLOPs, single-image inference latency, and peak memory usage to quantify computational efficiency in table 3.

SOTA Comparison: Table 4 compares SURGE with the Masked generative distillation (MGD) [20] baseline on SSDD. SURGE improves over MGD across all three detector families, with gains of +5.23, +1.63, and +22.34 mAP for Faster R-CNN, RetinaNet, and DETR, respectively. Unlike MGD, which distills knowledge by reconstructing teacher feature maps from randomly masked student features, SURGE performs teacher-guided region-level relational distillation. The proposed method transfers the relative geometry among object-region embeddings rather than enforcing dense feature-map recovery, making it better aligned with SAR ship detection and heterogeneous detector families.

Discussion: Overall, the results indicate that SURGE is particularly effective for detectors that rely on explicit region-level representations, such as two-stage architectures. By transferring relational geometry rather than enforcing local feature similarity, the proposed method enables compact student models to achieve near-teacher or teacher-surpassing performance with substantial reductions in model size. While

Table 3. Computational efficiency on SSDD.

Detector	Model	GFLOPs	Latency (ms)	Memory (MB)
Faster R-CNN	R101 Teacher	68.64	21.02	543.76
Faster R-CNN	R18 Student / Ours	49.77	10.53	362.52
RetinaNet	R101 Teacher	160.09	23.71	496.87
RetinaNet	R18 Student / Ours	127.31	13.32	316.72
DETR	R101 Teacher	44.36	22.50	315.63
DETR	R50 Student / Ours	24.97	15.80	243.61

Table 4. MGD [20] comparison on SSDD.

Detector	MGD [20] (mAP)	SURGE (mAP)
Faster R-CNN R18	62.80	68.03 (+5.23)
RetinaNet R18	58.70	60.33 (+1.63)
DETR R50	37.36	59.70 (+22.34)

gains for one-stage and transformer-based detectors are comparatively smaller, the consistent improvements across architectures highlight the generality of the proposed framework and its potential for efficient SAR ship detection under resource constraints.

6 Conclusion and Future Direction

We introduced the **SURGE**, the first relation-aware knowledge distillation framework for SAR ship detection that explicitly transfers the relational geometry of object representations from a high-capacity teacher detector to a lightweight student. By formulating distillation as a *student-anchored contrastive learning* problem in a shared embedding space, the proposed method goes beyond conventional feature or logit matching and enables the student to preserve the structural organization of the teacher’s representation space. The framework is *architecture-agnostic* and operates through a unified region-level distillation interface, allowing seamless application to two-stage, one-stage, and transformer-based detectors without modifying their core architectures. To the best of our knowledge, this work is also the first to demonstrate effective knowledge distillation for transformer-based SAR ship detectors, enabling relational transfer without relying on query-level supervision. Extensive experiments on the SSDD and HRSID benchmarks demonstrate that the proposed approach is particularly effective for two-stage detectors, where it achieves up to **6.2 mAP** and **8.0 AP₇₅** improvements over non-distilled students while reducing model size by more than **50%**. In several cases, the distilled student matches or surpasses teacher performance, highlighting the importance of transferring relational geometry for SAR imagery. For one-stage and transformer-based detectors, the method yields consistent but more modest gains, confirming its generality while revealing the varying impact of relational supervision across detector paradigms. Overall, this work establishes relation-aware distillation as a principled and scalable strategy for efficient SAR ship detection under resource constraints. Future work will explore extensions to multi-class SAR detection, stronger transformer architectures, and cross-modal distillation between SAR and optical domains.

References

- [1] Carion et al. 2020. End-to-end object detection with transformers. In *European conference on computer vision*. Springer, 213–229.
- [2] Chen et al. 2017. Learning efficient object detection models with knowledge distillation. *Advances in neural information processing systems* 30 (2017).
- [3] Feng et al. 2023. OEGR-DETR: A novel detection transformer based on orientation enhancement and group relations for SAR object detection. *Remote Sensing* 16, 1 (2023), 106.
- [4] Gao et al. 2022. RetinaNet-based compact polarization SAR ship detection. *IEEE Journal on Miniaturization for Air and Space Systems* 3, 3 (2022), 146–152.
- [5] Girshick et al. 2015. Fast r-cnn. In *Proceedings of the IEEE international conference on computer vision*. 1440–1448.
- [6] Han et al. 2024. Improving sar automatic target recognition via trusted knowledge distillation from simulated data. *IEEE Transactions on Geoscience and Remote Sensing* 62 (2024), 1–14.
- [7] Lang et al. 2025. Recent Advances in Deep Learning Based SAR Image Targets Detection and Recognition. *IEEE Journal of Selected Topics in Applied Earth Observations and Remote Sensing* (2025).
- [8] Lee et al. 2021. Privileged knowledge distillation for SAR building extraction. In *2021 IEEE International Geoscience and Remote Sensing Symposium IGARSS*. IEEE, 3014–3017.
- [9] Li et al. 2017. Ship detection in SAR images based on an improved faster R-CNN. In *2017 SAR in Big Data Era: Models, Methods and Applications (BIGSAR DATA)*. IEEE, 1–6.
- [10] Lin et al. 2017. Focal Loss for Dense Object Detection. In *Proceedings of the IEEE International Conference on Computer Vision (ICCV)*.
- [11] Min et al. 2019. A gradually distilled CNN for SAR target recognition. *IEEE access* 7 (2019), 42190–42200.
- [12] Moreira et al. 2013. A tutorial on synthetic aperture radar. *IEEE Geoscience and Remote Sensing Magazine* 1, 1 (2013), 6–43. doi:10.1109/MGRS.2013.2248301
- [13] Park et al. 2019. Relational knowledge distillation. In *Proceedings of the IEEE/CVF conference on computer vision and pattern recognition*. 3967–3976.
- [14] Tian et al. 2019. Contrastive representation distillation. *arXiv preprint arXiv:1910.10699* (2019).
- [15] Tung et al. 2019. Similarity-preserving knowledge distillation. In *Proceedings of the IEEE/CVF international conference on computer vision*. 1365–1374.
- [16] Wang et al. 2021. Boosting lightweight CNNs through network pruning and knowledge distillation for SAR target recognition. *IEEE Journal of Selected Topics in Applied Earth Observations and Remote Sensing* 14 (2021), 8386–8397.
- [17] Wang et al. 2021. SAR Target Classification Based on Knowledge Distillation. In *2021 CIE International Conference on Radar (Radar)*. IEEE, 2095–2098.
- [18] Wang et al. 2024. M-FSDistill: A feature map knowledge distillation algorithm for SAR ship detection. *IEEE Journal of Selected Topics in Applied Earth Observations and Remote Sensing* (2024).
- [19] Wu et al. 2018. Unsupervised feature learning via non-parametric instance discrimination. In *Proceedings of the IEEE conference on computer vision and pattern recognition*. 3733–3742.
- [20] Yang et al. 2022. Masked generative distillation. In *European Conference on Computer Vision*. Springer, 53–69.
- [21] Yang et al. 2022. SAR target recognition based on inverted residual and knowledge distillation. In *International Conference on Advanced Algorithms and Neural Networks (AANN 2022)*, Vol. 12285. SPIE, 210–217.
- [22] Yin et al. 2025. Ship detection transformer in SAR images based on key scattering points feature aggregation and context feature refinement. *IEEE Journal of Selected Topics in Applied Earth Observations and Remote Sensing* (2025).

[23] Yu et al. 2023. Multilevel adaptive knowledge distillation network for incremental SAR target recognition. *IEEE Geoscience and Remote Sensing Letters* 20 (2023), 1–5.

[24] Zhu et al. 2021. Deep learning meets SAR: Concepts, models, pitfalls, and perspectives. *IEEE Geoscience and Remote Sensing Magazine* 9, 4 (2021), 143–172.